CHEMICAL ENGINEERING TRANSACTIONS
VOL. 117, 2025
A publication of AIDIC
The Italian Association of Chemical Engineering
Online at www.cetjournal.it
Guest Editors: Fabrizio Bezzo, Flavio Manenti, Gabriele Pannocchia, Almerinda di Benedetto

ISBN 979-12-81206-17-5; **ISSN** 2283-9216
DOI: 10.3303/CET25117108

Simulation of the Power Generation Process of a Solid Oxide Fuel Cell Powered by Green Hydrogen from an Alkaline Water Electrolysis

Pedro C Dias[a], Alexander Polasek[b], José G. M. Furtado[b], Alexandre V. Grillo[c], Roberto B. de Carvalho[a], Brunno F. dos Santos[a,*]

[a]Department of Chemical and Material Engineering (DEQM). Pontifical Catholic University of Rio de Janeiro (PUC-Rio). Rua Marquês de São Vicente, 225 – Gávea, Rio de Janeiro – RJ, 22430-060, Brazil.
[b]Department of Energy Transition and Sustainability, Electric Energy Research Center (CEPEL), Av. Horácio Macedo, 354 - University City of the Federal University of Rio de Janeiro, Rio De Janeiro, 21941-911, Brazil
[c]Department of Physical Chemistry Federal Institute of Education, Science and Technology (IFRJ), Rua Lúcio Tavares, 1045 – Centro, Nilópolis – RJ, 26530- 060, Brazil.
bsantos@puc-rio.br

Fossil fuels currently meet 80% of global energy demand, significantly contributing to greenhouse gas (GHG) emissions, such as CO_2 and CH_4. To address this challenge, there is a growing interest in sustainable energy sources with lower environmental impact, such as green hydrogen. This study aims to simulate the performance of a solid oxide fuel cell (SOFC) powered by green hydrogen from alkaline water electrolysis (AEW) and air. Simulations were conducted using Aspen Plus for thermodynamic modeling and Excel for data analysis, exploring different operating temperatures and pressures. Key performance metrics, including polarization curves, power density, and efficiency for the SOFC, and H_2 production and voltaic efficiency for the AEW, were evaluated. The results demonstrated optimal conditions at 90 °C and 5 bar for AEW and at 1000 °C and 10 bar for SOFC, achieving an electrical efficiency of 66.63% and a required power input of 9.57 kW for AEW. These findings underscore the feasibility of integrating green hydrogen production and high-efficiency SOFCs for sustainable power generation.

1. Introduction

The increasing global energy demand and the pressing need to address environmental concerns have sparked significant interest in sustainable energy solutions. Fossil fuels like coal, natural gas, and oil currently account for 80% of global energy consumption, releasing greenhouse gases (GHGs) such as carbon dioxide (CO2) and methane (CH4). These emissions are linked to severe environmental challenges, including climate change, ozone layer depletion, acidification, and air pollution, prompting global efforts to reduce reliance on fossil fuels (de Fátima Palhares et al., 2018; Cartaxo et al., 2021).Hydrogen has emerged as one of the most promising alternatives for renewable and environmentally friendly energy due to its abundance in the universe. However, its availability on Earth is limited to chemically bonded forms in water, fossil fuels, and biomass, necessitating chemical processes for its production. Hydrogen is classified into various "colors," such as blue, gray, black, and green, depending on the production technology and its environmental impact. Among these, green hydrogen, produced via water electrolysis powered by renewable electricity, offers a carbon-free pathway for sustainable energy systems (Kumar and Lim, 2022).Alkaline water electrolysis (AEW) is one of the most established technologies for green hydrogen production. Operating at low temperatures, it utilizes a concentrated alkaline solution and nickel-coated stainless-steel electrodes, with porous diaphragms facilitating the transport of hydroxide ions (OH^-) (Kumar and Lim, 2022).Fuel cells complement green hydrogen by efficiently converting its chemical energy into electricity through redox reactions, producing no harmful emissions or noise. Among various fuel cell types, solid oxide fuel cells (SOFCs) are distinguished by their high operating temperatures, which enable direct reforming of hydrocarbon-based fuels like methanol and natural gas. This

Paper Received: 7 December 2024; Revised: 13 April 2025; Accepted: 24 May 2025
Please cite this article as: Dias P.C., Polasek A., Furtado J.G.M., Grillo A.V., de Carvalho R.B., dos Santos B.F., 2025, Simulation of the Power Generation Process of a Solid Oxide Fuel Cell Powered by Green Hydrogen from an Alkaline Water Electrolysis, Chemical Engineering Transactions, 117, 643-648 DOI:10.3303/CET25117108

characteristic, combined with their resistance to fuel contaminants like CO and the possibility of utilizing residual heat for cogeneration, makes SOFCs highly efficient. Typically, SOFCs use yttria-stabilized zirconia (YSZ) as the electrolyte, with $La_{0.8}Sr_{0.2}MnO_3$ (LSM) as the cathode and a cermet of NiO-YSZ as the anode (Corigliano et al., 2022).This study aims to simulate and evaluate the performance of an SOFC system generating 4 kW of power, fueled by green hydrogen produced via AEW. Simulations were conducted under various operating temperatures and pressures for both the SOFC and AEW systems. Key performance metrics, including thermal and electrical efficiency for the SOFC, as well as voltaic efficiency and power requirements for the AEW, were analyzed to assess the potential of this integrated approach to sustainable energy generation. The objective is to identify a more optimized system configuration that enhances overall efficiency and performance.

2. Methodology

This study simulated the solid oxide fuel cell (SOFC) powered by green hydrogen from an alkaline electrolysis of water (AEW) and air, AEW-SOFC simulation. The simulations were conducted using Aspen Plus 14.0 for thermodynamic modeling and Excel for data analysis. They were performed across various operating temperatures and pressures, with the SOFC evaluated at 600, 800, and 1000 °C and pressures of 3, 6.5, and 10 bar, while the AEW was analyzed at 60, 75, and 90 °C and pressures of 5, 7, and 9 bar.
This global reaction occurring in the AEW is represented by Eq(1):

$$H_2O \rightarrow H_2 + \frac{1}{2}O_2 \quad (1)$$

The actual voltage of the electrolytic cell (V_{ec}) is calculated using operating parameters such as temperature (T) in °C, the current density of the electrolyte cell (j_{ec}) in $A.m^{-2}$, the operating pressure (p) in bar, and the standard potential of the hydrogen cell (V^0) in V, as well as the operating coefficients of the electrolytic cell (r_1, r_2, d_1, d_2, s, t_1, t_2, t_3), their values are $4{,}445.10^{-5}$ Ω.m², $6{,}89.10^{-9}$ Ω.m².°C^{-1}, -3,13 Ω.m², 4,47 Ω.m².bar^{-1}, 0,34 V, -0,0154 m².A^{-1}, 2,002 m².°C.A^{-1} e 15,24 m².°C.A^{-1}, respectively, as shown in Eq(2) below (Sánchez et al., 2020).

$$V_{ec} = V^0 + [r_1 + d_1 + r_2T + d_2p]j_{ec} + slog\left[\left(t_1 + \frac{t_2}{T} + \frac{t_3}{T^2}\right)j_{ec} + 1\right] \quad (2)$$

The definition of the electrolytic cell's power (P_{ec}) is provided in Eq(3) below, where A_{ec} is the electrolytic cell area in m² and N_{ec} is the number of electrolytic cells (Sánchez et al., 2020).

$$P_{ec} = V_{ec}N_{ec}A_{ec}j_{ec} \quad (3)$$

Furthermore, one of the key metrics for evaluating the performance of the electrolytic cell is the Faraday efficiency (n_F), an index that varies from 0 to 100% and gauges the production quality concerning the electrolytic cell's target product, in this case, H_2. It is computed as follows, in Eq(4). Where f_{11}, f_{12}, f_{21}, f_{22} are operational coefficients and their values are 478645,74 A².m^{-4}, -2953,15 A².m^{-4}.°C^{-1}, 1,0396 and -0,00104 °C^{-1}, respectively (Kelly, 2014).

$$\eta_F = \left(\frac{j_{ec}^2}{f_{11} + f_{12}T + j_{ec}^2}\right)(f_{21} + f_{22}T) \quad (4)$$

The molar quantity of hydrogen produced, and consequently the amount of water converted based on the stoichiometry of the cell's overall reaction, can be determined using the actual potential, power, and Faraday efficiency of the electrolytic cell. This relationship is expressed in Eq(5), where F is Faraday's constant and n_{e^-} is the number of electrons transferred during the electrolysis process (Sánchez et al., 2020).

$$n_{H_2} = n_{H_2O} = \frac{P_{ec}}{V_{ec}n_{e^-}F}\eta_F \quad (5)$$

Furthermore, the voltaic efficiency (η_v), which is an index that goes from 0 to 100% and calculates the ratio of the electrolysis's operational voltage to thermoneutral voltage, is another crucial metric for assessing the electrolytic cell's performance. This is illustrated in Eq(6) below, where V_{tm} is the thermoneutral voltage and its value is 1,481 V (Harrison et al., 2010).

$$\eta_v = \frac{V_{tm}}{V_{ec}} \quad (6)$$

The global reaction occurring in the SOFC is represented by Eq(7):

$$H_2(gas, anode) + \frac{1}{2}O_2(gas.cathode) \rightarrow H_2O(gas, anode) \quad (7)$$

The ideal potential of the SOFC is determined by the Nernst equation, Eq(8). Where E^0 is the standard potential, R is the universal gas constant, and P_{H2}, P_{O2}, and P_{H2O} are the partial pressures of the corresponding species (Corigliano et al., 2022).

$$E_{rev} = E^0 - \frac{RT}{2F}\, ln\left(\frac{p_{H_2O}}{p_{H_2} p_{O_2}^{\frac{1}{2}}}\right) \tag{8}$$

However, the actual potential is reduced due to losses such as activation, ohmic, and concentration overpotentials. These losses are considered using Eq(9) (Corigliano et al., 2022).

$$V_{fc} = E_{rev} - \eta_{at} - \eta_{ohm} - \eta_{conc} \tag{9}$$

The activation overpotential (η_{at}) arises from the rate of irreversible chemical reactions occurring on the electrode surface. Although the Butler-Volmer equation provides a comprehensive model for calculating activation losses, it is inherently non-linear and computationally demanding. A simplified version, known as the Tafel equation, is often used, but it is only applicable when $j^{fc} > 4j_0$. To address this limitation, a modified form of the equation is applied, as shown in Eq(10). This modification assumes that the cathodic transfer coefficient is equal to the anodic transfer coefficient, simplifying the calculation while maintaining accuracy under the specified conditions (Gebregergis et al., 2008).

$$\eta_{at} = \frac{RT}{2\alpha F} ln\left(\frac{j^{fc}}{2j_0} + \sqrt{\left(\frac{j^{fc}}{2j_0}\right)^2 + 1}\right) \tag{10}$$

Here, α represents the charge transfer coefficient, which quantifies the fraction of the applied electrical energy that drives the electrochemical reaction. Its value ranges from 0 to 1 and is typically assumed to be constant, with a standard value of 0.5. jfc denotes the current density, while j0 refers to the exchange current density, which is determined using Eq(11). In this equation, 120 kJ/mol is the activation energy of the electrochemical reaction and A=101.2 kA/cm2 is a pre-exponential factor (Gebregergis et al., 2008).

$$j_0 = Ae^{-\frac{E_{act}}{RT}} \tag{11}$$

The ohmic overpotential arises from the resistance of materials to the flow of electric charge within the fuel cell. This resistance results in energy losses that are proportional to the specific area resistance (r) of the material and the current density (j), as described by Eq(12). Where γ = 0.2 Ω.cm², β = −2870 K, and T_0 = 973 K are the constant coefficients of the fuel cell (Gebregergis et al., 2008).

$$\eta_{ohm} = \; rj = \gamma e^{\beta\left(\frac{1}{T_0} - \frac{1}{T}\right)} j^{fc} \tag{12}$$

Concentration losses within the fuel cell primarily result from the diffusion and solubilization processes of reactive species, as well as the transport limitations of gaseous substances through the porous electrodes. These losses become significant at high current density values. Typically, when the thicknesses and microstructures of the cathode and anode are comparable, the concentration polarization at the anode is significantly smaller than that at the cathode. Consequently, the overall concentration losses are predominantly influenced by the cathode, and their magnitude can be calculated using the appropriate mathematical relationship described in Eq(13) (Shingal and Kendall, 2003).

$$\eta_{conc} = -\frac{RT}{2F} ln\left(1 - \frac{j^{fc}}{j_{cs}}\right) \tag{13}$$

Here, j_{cs} represents the limiting current density of the cathode, which is determined by the diffusion characteristics of the system, Eq(14). This parameter is influenced by $D_{c(eff)}$, the effective gas diffusivity through the cathode, l_c, the thickness of the cathode, and p_{o2}, the partial pressure of oxygen in the oxidant. These variables collectively define the cathode's ability to transport reactive gases and are critical in assessing the fuel cell's performance under high current density conditions (Shingal and Kendall, 2003).

$$j_{cs} = \frac{4F p_{o_2} D_{c(eff)}}{\left(\frac{p - p_{o_2}}{p}\right) RT l_c} \tag{14}$$

The evaluation of performance is based on electrical and thermal efficiencies. They are calculated using the ratio of the chemical power of the incoming fuel to its electrical or thermal power, as shown in Eq(15) and Eq(16) below (Corigliano et al., 2022).

$$\eta_{el} = \frac{n_c V_c^{fc} i^{fc}}{\sum_f n_c m_{in,f} LHV_{r,f}} \tag{15}$$

$$\eta_{th} = \frac{-\frac{n_c i^{fc}}{2F}\left[\Delta\tilde{h}_{r,f} + \left(2FV_c^{fc}\right)\right]}{\sum_f n_c m_{in,f} LHV_{r,f}} \tag{16}$$

Where n_c is the number of cells, $\Delta\tilde{h}_r$ is the reaction enthalpy of the fuel fed and its value for hydrogen is -286 kJ/mol, LHV_r represents the lower heating value of the fuel and its value for hydrogen is 120.10^6 J/kg and m_{in} represents the mass flow rate and can be calculated as shown in Eq(17) below, where MW_{H2} is the molecular weight of the H_2 and U_f is the fuel utilization factor (Corigliano et al., 2022).

$$m_{H_2} = \frac{i^{fc} MW_{H_2}}{2U_f F} \tag{17}$$

3. Results and discussion

The AEW-SOFC simulations was performed as shown in Figure 1 bellow.

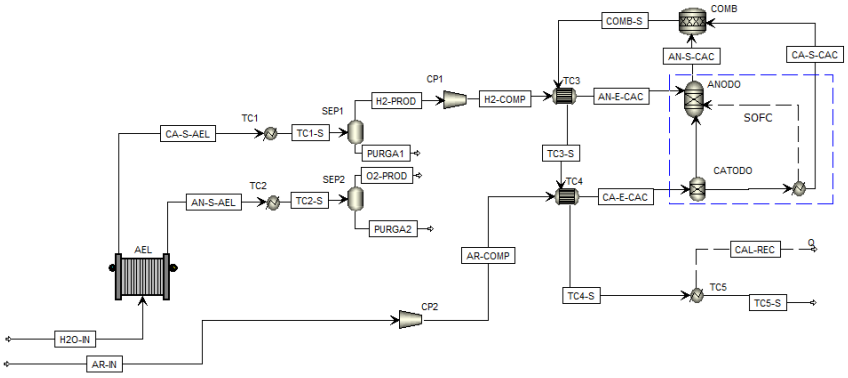

Figure 1: Simulation process of AEW-SOFC in Aspen Plus.

The AEW structure was modeled based on Sánchez et al. (2020), and the SOFC system was developed following the framework proposed by Bendaikha-Touafek et al. (2007). In the AEW module, water undergoes alkaline electrolysis, accompanied by electrolyte recycling. The resulting streams, primarily composed of hydrogen and oxygen, are then cooled using a heat exchanger and purified in a separator.
Subsequently, the hydrogen and air streams are compressed to increase their pressure. Their temperatures are elevated by passing them through heat exchangers, where energy integration is achieved by utilizing heat from the exhaust gases of the combustor. Once preheated, the streams enter the SOFC, with hydrogen directed to the anode and air to the cathode. The remaining hydrogen exiting the SOFC is burned in the combustor to produce H_2O. For simplicity, the electrolyte is not explicitly modeled in this system; however, its effects are incorporated through the loss parameters. Finally, a heater is employed to recover energy in the form of heat, further optimizing the system's efficiency.

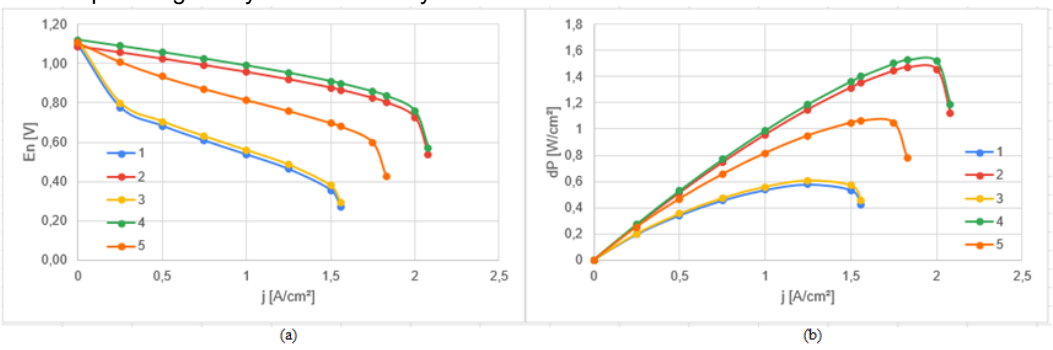

Figure 2: The (a) polarization curve and (b) power density curve for the five scenarios.

The SOFC generation power was set at 4 kW, and five different scenarios were analyzed under different combinations of temperature and pressure. They were at 600 °C and 3 bar, 1000 °C and 3 bar, 600 °C and 10

bar, 1000 °C and 10 bar, and 800 °C and 6.5 bar, named 1, 2, 3, 4 and 5, respectfully. Based on these simulations, polarization curves and power density were evaluated, with their results illustrated in Figure 2, while electrical and thermal efficiency were assessed and presented in Figure 3.

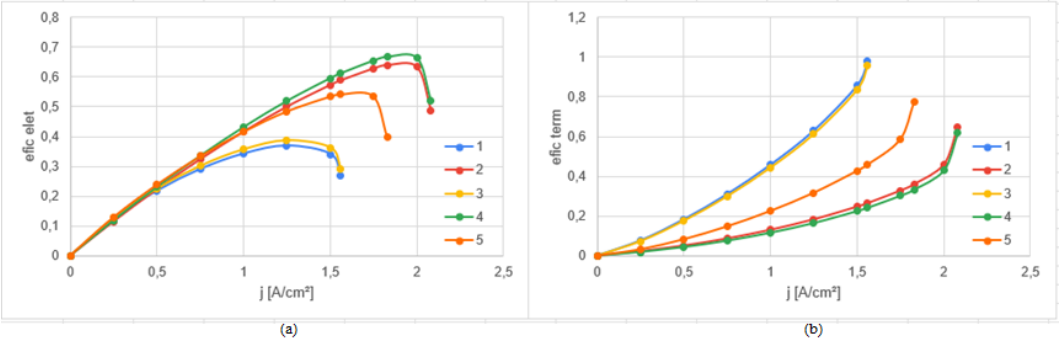

Figure 3: The (a) electrical and (b) thermal efficiency curves for the five scenarios.

The results demonstrated that increasing the SOFC operating temperature led to significant improvements in polarization and power density curves, while thermal efficiency exhibited a slight decline. This behavior was expected since higher temperatures directly influence overpotential values but have a limited impact on theoretical potential. Similarly, increasing the operating pressure of the SOFC resulted in minor performance improvements across most metrics, except for thermal efficiency, which remained largely unaffected. Intermediate values of temperature and pressure produced corresponding intermediate outcomes.
The AEW simulations followed a similar approach, with five scenarios created under different operating conditions: 60 °C and 5 bar, 90 °C and 5 bar, 60 °C and 9 bar, 90 °C and 9 bar, and 75 °C and 7 bar. Each AEW scenario was paired with each SOFC scenario, and the results are summarized in Table 1.

Table 1: Results from the scenarios simulated setting the SOFC generation power equal to 4 kW.

T_{AEL} (°C)	P_{AEL} (bar)	T_{SOFC} (°C)	P_{SOFC} (bar)	n_{H2O} (kmol/h)	n_f	P_{ec} (kW)	n_{volt}
60	5	600	3	0,162	0,9455	18,14	0,7476
90	5	600	3	0,162	0,9241	17,31	0,8015
60	9	600	3	0,162	0,9455	18,19	0,7456
90	9	600	3	0,162	0,9241	17,36	0,7992
75	7	600	3	0,162	0,9349	17,76	0,7724
60	5	1000	3	0,093	0,9455	10,45	0,7476
90	5	1000	3	0,093	0,9241	9,97	0,8015
60	9	1000	3	0,093	0,9455	10,47	0,7456
90	9	1000	3	0,093	0,9241	10,00	0,7992
75	7	1000	3	0,093	0,9349	10,23	0,7724
60	5	600	10	0,154	0,9455	17,29	0,7476
90	5	600	10	0,154	0,9241	16,50	0,8015
60	9	600	10	0,154	0,9455	17,34	0,7456
90	9	600	10	0,154	0,9241	16,55	0,7992
75	7	600	10	0,154	0,9349	16,93	0,7724
60	5	1000	10	0,089	0,9455	10,03	0,7476
90	5	1000	10	0,089	0,9241	9,57	0,8015
60	9	1000	10	0,089	0,9455	10,06	0,7456
90	9	1000	10	0,089	0,9241	9,60	0,7992
75	7	1000	10	0,089	0,9349	9,82	0,7724
60	5	800	6,5	0,110	0,9455	12,33	0,7476
90	5	800	6,5	0,110	0,9241	11,77	0,8015
60	9	800	6,5	0,110	0,9455	12,36	0,7456
90	9	800	6,5	0,110	0,9241	11,80	0,7992
75	7	800	6,5	0,110	0,9349	12,07	0,7724

The table shows that an increase in AEW temperature leads to slightly better results, while an increase in AEW pressure causes a slight deterioration. The variation in SOFC temperature leads to better results, and an increase in SOFC pressure also results in slightly better results. Intermediate pressure and temperature values in both AEW and SOFC result in intermediate results. With this, the best results found were with the AEW at 90 °C and 5 bar and the SOFC at 1000 °C and 10 bar, where an electrical efficiency in the SOFC of 66.63% and a necessary power in the AEW of 9.57 kW were obtained.

4. Conclusions

The analyses in this study determined the optimal operating conditions for maximizing overall efficiency and performance: AEW at 90 °C and 5 bar, and SOFC at 1000 °C and 10 bar. Under these conditions, the SOFC achieved an electrical efficiency of 66.63%, while the AEW required a power input of 9.57 kW. Notably, similar results were observed under the same AEW conditions when the SOFC operated at 1000 °C and 3 bar. This highlights the need for a comprehensive economic analysis to determine the most cost-effective scenario, taking into account not only system efficiencies but also operational and capital costs. Future studies should focus on this aspect to further optimize the integration of AEW and SOFC systems for sustainable energy generation.

Nomenclature

A_{ec} – electrolytic cell area
$D_{c(eff)}$ – effective gas diffusivity through the cathode
E^0 – standard potential of the fuel cell
E_{rev} – ideal potential of a fuel cell
F – Faraday's constant
f_{11}, f_{12}, f_{21}, f_{22} – operational coefficients
j^0 – exchange density
j_{cs} – limiting current density of the cathode
j^{ec} – current density of the electrolyte cell
j^{fc} – current density of the fuel cell
l_c – thickness of the cathode
LHV_r – lower heating value of the fuel
m – mass flow rate
MW_{H2} – molecular weight
n_c – number of cells
n_{H2} – molar amount of hydrogen produced
n_{H2O} – molar amount of water converted
p – operational pressure
P_{ec} – electrolyte cell's power
P_{H2}, P_{O2}, P_{H2O} – partial pressures of the corresponding species
p_{O2} – typical partial pressure of oxygen in the oxidant
R – universal gas constant
r – specific area constant
r_1, r_2, d_1, d_2, s, t_1, t_2, t_3 – operational coefficients of the electrolytic cell
T – operational temperature
U_f – fuel utilizational factor
V^0 – standard potential of the electrolytic cell
V_{ec} – voltage of the electrolytic cell
V_{fc} – real potential of the fuel cell
V_{tm} – thermoneutral voltage
α – charge transfer coefficient
γ, β, T_0 – constant coefficients of the fuel cell
$\Delta\tilde{h}_r$ – reaction enthalpy of the fuel fed
η_{at} – activation overpotential
η_{conc} – concentration overpotential
η_{ele} – electrical efficiency
η_F – Faraday efficiency
η_{term} – thermal efficiency
η_{ohm} – ohmic overpotential
η_v – voltaic efficiency

Acknowledgments

Thanks to CNPq/MCT, CAPES, FAPERJ (E-26/200.282/2023-283570), IFSULDEMINAS, and FINEP for the financial support to the Department of Chemical and Materials Engineering (DEQM) at the PUC-Rio. And ANEEL and CEPEL for their financial support and in the preparation of this article.

References

Bendaikha-Touafek W., Touafek K., Serir L., 2007, Operation of a total energy system based on SOFC fuel cell, Proceedings of the 2IWH, Ghardaïa, Algeria.

Cartaxo M., Fernandes J., Gomes M., Pinho H., Nunes V., Coelho P., 2021, Hydrogen Production via Wastewater Electrolysis—An Integrated Approach Review, Proceedings of the International Conference on Smart City Applications, Springer International Publishing, Cham, Switzerland, 671-680.

Corigliano O., Pagnotta L., Fragiacomo P., 2022, On the technology of solid oxide fuel cell (SOFC) energy systems for stationary power generation: A review, Sustainability, 14(22), 15276.

de Fátima Palhares D.D.A., Vieira L.G.M., Damasceno J.J.R., 2018, Hydrogen production by a low-cost electrolyzer developed through the combination of alkaline water electrolysis and solar energy use, International Journal of Hydrogen Energy, 43(9), 4265-4275.

Gebregergis A., Pillay P., Bhattacharyya D., Rengaswemy R., 2008, Solid oxide fuel cell modelling, IEEE Transactions on Industrial Electronics, 56(1), 139-148.

Harrison K.W., Remick R., Martin G.D., Hoskin A., 2010, Hydrogen production: fundamentals and case study summaries, Hydrogen Fuel Cells, 207-226.

Kelly N.A., 2014, Hydrogen production by water electrolysis, In Advances In: Advances in Hydrogen Production, Storage and Distribution, Woodhead Publishing, Cambridge, UK, 159-185.

Kumar S.S.; Lim H., 2022, An overview of water electrolysis technologies for green hydrogen production, Energy reports, 8, 13793-13813.

Sánchez M., Amores E., Abad D., Rodríguez L., Clemente-Jul C., 2020, Aspen Plus model of an alkaline electrolysis system for hydrogen production, International Journal of Hydrogen Energy, 45(7), 3916-3929.

Singhal S.C., Kendall K. (Eds), 2003, High-temperature solid oxide fuel cells: Fundamentals, design and applications, Elsevier, Amsterdam, Netherlands.